ingegneria sismica
International Journal of Earthquake Engineering
Anno XLIII - Num. 1 - 2026

Research on the coupling mechanism of trajectory planning and task allocation for eVTOL multi-aircraft cooperative emergency distribution under low-altitude economic scenario

Hongyu Jia[1,2], *Jianhua Zhang*[1,*], *Lulu Zhang*[3] *and Yarui Gao*[1]

[1] School of Management, Zhengzhou University, Zhengzhou, Henan, 450001, China
[2] School of Art & Design, Zhengzhou University of Light Industry, Zhengzhou, Henan, 450002, China
[3] School of Information Engineering, Zhengzhou University of Technology, Zhengzhou, Henan, 450044, China

SUMMARY: *Aiming at the problem of trajectory planning and task allocation for eVTOL multi-aircraft cooperative emergency delivery in low-altitude economic scenarios, a two-layer planning model nested in each other is proposed. The upper layer model makes task allocation decisions at the macro level, and is modeled with the objective function of minimizing the total delivery time, and two solution algorithms are designed based on the ant colony algorithm according to two commonly used task allocation ideas. In the lower level, the objective is to minimize the total cost of multi-UAVs to perform the mission, establish the spatio-temporal coordination mechanism, and introduce the quantum genetic algorithm to solve the eVTOL multi-UAV trajectory planning by combining with the task allocation decision of the upper level model. Finally, simulation analysis is carried out, and the results show that the paths planned by this paper's method are shortened by at least 6.4% compared with the GWO model. Compared with the traditional genetic algorithm, the average value of the total cost of synergy of the quantum genetic algorithm used is optimized by 1.66%. In the planning environment of this paper, the algorithm solution efficiency and quality are optimal when the cost weights of each sub-objective are 0.45 and 0.65, respectively, and the population size is 200.*

KEYWORDS: *ant colony algorithm; quantum genetic; task allocation; trajectory planning; eVTOL*

1 Introduction

In December 2023, China for the first time fixed the low-altitude economy as a strategic emerging industry [1]. Literature [2], in the context of low altitude economy as China's national strategy, sorted out the core theoretical connotations of low altitude economy and new quality productivity, and deeply analyzed the intrinsic logical connection between the two. With the rapid development of key technologies such as autonomous driving, artificial intelligence, battery, flight control, and autonomous obstacle avoidance, electric vertical take-off and landing (eVTOL) vehicles have become a fit for the low-altitude economy scenario due to their advantages of easing traffic congestion, occupying a small area, shortening travel time, and reducing air pollution [3-6]. eVTOL vehicles, as an effective vehicle for the low-altitude intelligent transport system The eVTOL vehicle as an effective carrier of low-altitude intelligent

*tjzhangjianhua@163.com
https://doi.org/10.65102/is2026232
Published: 30 April, 2026

transportation system is in line with the “green revolution” trend of low-carbon and sustainable development [7, 8].

Regarding the research on the application of eVTOL vehicles and their related fields under low-altitude economy, literature [9], based on the examination of the background of low-altitude economic development, overviewed the historical evolution and current research status of eVTOL vehicles, especially in the aspects of flight performance indexes, intelligent and autonomous flights, etc., and analyzed in depth the prospects of the sustainable development and commercialization of eVTOLs under the complex urban environments. Literature [10] discusses the elements of low-altitude economic development and traffic management by sorting out the connotation of low-altitude economy, transportation, and traffic management, and studies the forms of management of low-altitude manned aircrafts, UAVs, and urban air mobility. Literature [11] explores the contribution of eVTOL vehicles to the low-altitude economy, emphasizes that eVTOL vehicles reshape the transportation system, shorten travel times, and analyzes the differences between them and traditional modes of transportation. Literature [12] discusses eVTOL machine technology and its impact on urban development and explores the main designs, advantages and barriers currently being developed, as well as the challenges posed by civil certification. Literature [13] provides an overview of recent improvements in eVTOL machines, in particular the basic research and current state of the art of materials used in core components such as power cell systems and motors.

Compared with traditional vehicles, the advantages of eVTOL vehicles include the use of electric propulsion systems to reduce atmospheric pollution; the use of distributed electric drive technology to reduce operational noise; the realization of autonomous flight with the help of a flight control system; the simplified structural design and easy maintenance features that can reduce operational costs; and a high degree of safety and reliability [14-17]. These characteristics together provide a solid foundation for the application of eVTOL aircraft in the modern transportation field, making it widely used in the field of emergency distribution [18].

The application of eVTOL vehicles in emergency distribution has many advantages and some limitations. Literature [19] compared eVTOL vehicles and UAVs with traditional ground transportation methods with the aim of examining the feasibility of an innovative aerial transportation system for blood-derived medications in emergency situations, emphasizing the superiority of eVTOL vehicles. Literature [20] investigated the applicability of eVTOL in emergency medical transportation and used the Brazilian Amazon as a case study, showing that eVTOL can cover a wide area from a few operational bases, but that more bases need to be strategically distributed to achieve similar population coverage. Literature [21] describes the potential application of eVTOL vehicles in emergency medical services and describes its advantages and limitations, and proposes a methodology for identifying vertical harbors of healthcare networks in order to improve the coverage of emergency medical services in hard-to-reach areas.

Emergency distribution, such as natural disasters, public health events, traffic accidents, etc., rapid, stable and efficient distribution of emergency supplies is crucial, and in order to ensure that emergency supplies can reach their destinations in time, a single vehicle, although it has the advantages of high covertness and simple control, is unable to satisfy the complex environment and mission requirements [22-25]. Multi-vehicle synergy can precisely make up for the shortcomings of a single vehicle. Task assignment and trajectory planning are the key technologies of multi-copter synergy, which are directly related to the safety, economy and environmental impact of flight. In emergency distribution, eVTOL multi-copter synergistic emergency distribution trajectory planning and task assignment can quickly establish an airborne life channel and improve the efficiency of rescue in the case of road damage [26-29]. Therefore, an in-depth study of the coupling mechanism of trajectory planning and task

allocation for eVTOL multi-copter cooperative emergency distribution has important application value and theoretical significance.

In the research related to eVTOL multi-copter cooperative trajectory planning and task assignment, literature [30] proposed an ant colony optimization algorithm based on adaptive parameter adjustment and two-way search in order to quickly plan the effective trajectory of eVTOL vehicle, which can effectively plan a reasonable trajectory compared with other algorithms, and also solves the uncertainty problem, improving the eVTOL vehicle multi-copter cooperative capability. Literature [31] reviewed from path planning and scheduling algorithms, emergency response decision support system, low altitude economy and urban air traffic management, etc. The results show that the eVTOL vehicle emergency delivery technology has been developed from single-aircraft application to intelligent multi-modal collaborative system, which shows obvious advantages in emergency distribution. Literature [32] highlights the significant advantages of eVTOL vehicles in disaster relief distribution, but the uncertainty of environment and demand constrains the collaborative performance of multiple aircraft, for which a new robust optimization model and a multi-UAV mission planning method combining two improved intelligent algorithms are proposed.

The eVTOL multi-UAV collaborative tasking and path planning, which do not exist in isolation, must be considered in a coupled relationship so as to conduct an integrated study. In this paper, a two-layer planning model for eVTOL multi-drone cooperative emergency distribution is constructed. The upper layer model is based on the ant colony algorithm to design the task allocation method that allows transit and the task allocation method that does not allow transit. For the lower-layer emergency logistics task eVTOL multi-aircraft cooperative trajectory static planning problem, a spatio-temporal coordination mechanism is established, combined with the task allocation scheme of the upper-layer model, and optimized and solved by quantum genetic algorithm. The method generates a designated candidate path for each UAV in the cluster for spatio-temporal coordination, which can realize that multiple UAVs can reach the target area at the same time at the same cost by avoiding obstacles and avoiding collisions throughout the whole process from different starting points.

2 eVTOL Multi-machine Collaborative Emergency Distribution Problem Model and Algorithm

Aiming at the eVTOL multi-aircraft object emergency distribution problem, this paper establishes a two-layer planning model. The upper layer planning model is used to solve the task allocation problem, i.e., it mainly solves the distribution order of UAVs to each demand point as well as the distribution scheme of goods. The lower layer planning model is used to solve the eVTOL multi-machine path planning problem, i.e., the optimal path for eVTOL multi-machine distribution is calculated according to the task allocation scheme. Upper layer planning and lower layer planning are interconnected and interact with each other.

2.1 eVTOL multi-machine tasking model

In this paper, there are material distribution points (i.e., relief points) and several demand locations in a disaster-stricken area, and the number of people in each demand location is different, and the demand for materials is also different. Now it is necessary to reasonably design the UAV scheduling program, so that multiple UAVs can cooperate in distribution and efficiently distribute the relief materials to the demand locations.

2.1.1 Upper layer model construction

T is the total time spent after completing all the distribution tasks, i is the number of the relief point, j, l is the number of the demand point, m is the number of times spent on completing the distribution of the demand point j, n is the number of demand points, t_j is the total time spent on completing the distribution of the demand point j, t_{jr} is the time spent on distributing the demand point j for the r th time, t_{ij} is the time spent by the drone flying from the relief point i to the demand point j, t_{il} is the time spent by the drone flying from the relief point i to the demand point l, t_{lj} is the time spent by the drone flying from the demand point l to the demand point j, q_j is the amount of demand from the demand point j, x_{ij} is the amount of total UAV delivery from relief point i to demand point j, x_{lj} is the total UAV delivery from demand point l to demand point j, y_{ijr} is the UAV's r th delivery from relief point i to demand point j, d_{ij} is the distance from relief point i to demand point j, d_{lj} is the distance from demand point l to demand point j, $C_{\max}$ is the maximum loading capacity of the UAV, and $S_{\max}$ is the maximum range of the UAV.

$$T = \min\left(\max\{t_j, j = 1, 2, \ldots, n\}\right) \tag{1}$$

where t_j is calculated as:

$$t_j = \sum_{r=1}^{m} t_{jr} \tag{2}$$

The computation of t_{jr} varies depending on how the tasks are assigned:

$$\text{Transit not permitted: } t_{jr} = t_{ij} \tag{3}$$

$$\text{Transit permitted: } t_{jr} = \begin{cases} t_{il} + t_{lj}, & t_{il} > t_{ij} \\ t_{ij} + t_{lj}, & t_{il} \le t_{ij} \end{cases} \tag{4}$$

$$q_j = x_{ij} + \sum_{l=1, l\neq j}^{n} x_{lj},\ j = 1, 2, \ldots, n \tag{5}$$

$$y_{ijr} \le C_{\max} \tag{6}$$

$$t_j = 0, d_{ij} + d_{lj} \ge S_{\max}/2 \tag{7}$$

$$t_j = 0, d_{ij} \ge S_{\max}/2 \tag{8}$$

The objective function Eq. (1) indicates that the time to minimize the last completed task, i.e., the overall distribution time is the shortest. Equation (5) indicates that the supplies distributed to j from each location must satisfy its demand. Eq. (6) indicates that the amount of supplies distributed at each time must not be greater than the maximum loading capacity of

the UAV. Equations (7) and (8) ensure that the remaining power of the UAV for one mission is sufficient for the return trip.

2.1.2 Representation of allocation schemes

The task allocation methods used in this paper are shown in Fig. 1, one of which is a distribution method in which all UAVs are directly distributed without involving mutual transit between demand locations, consistent with the distribution method shown in Fig. 1(a). The second is a distribution method that allows UAVs to transit between demand locations, consistent with the distribution method shown in Fig. 1(b).

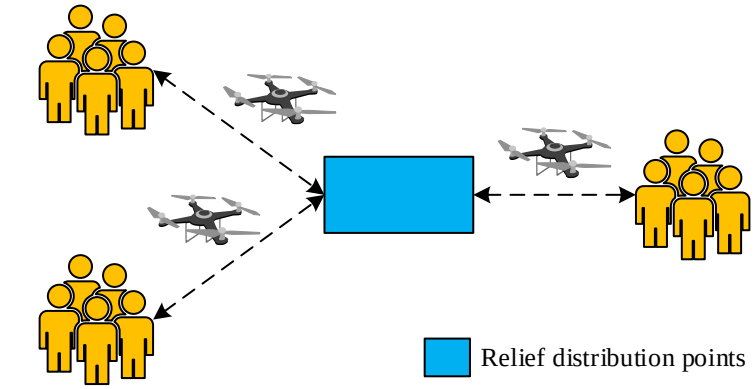

(a) Delivery methods not permitting transhipment

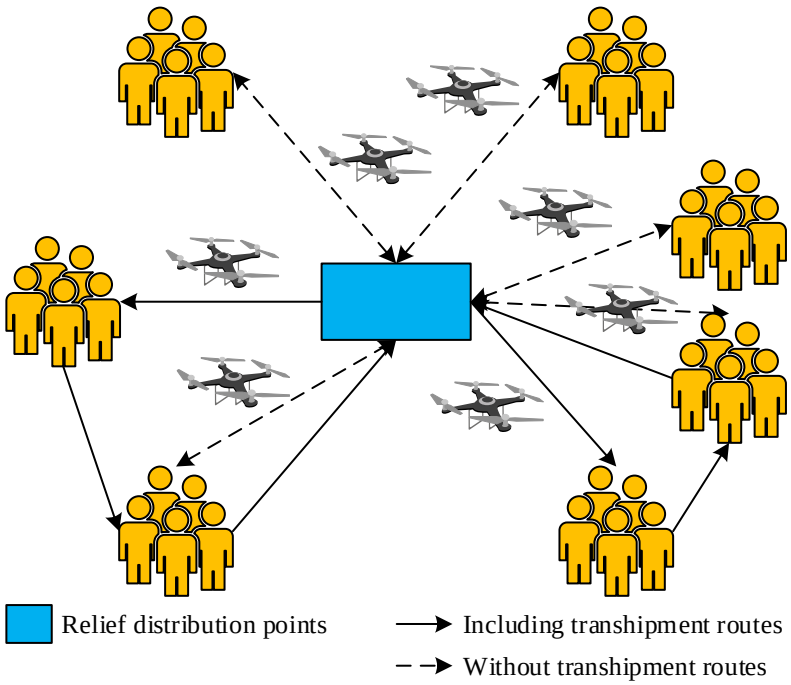

(b) Delivery methods permitting transhipment

Figure 1: Way of delivery of drones

In addition, the basic data used in this paper include the location information of the relief point and the demand point, the load and range parameters of the UAV, and the number of

people at each demand point, through which the number of people at the demand point can be set to its demand for supplies. Based on the above data, a UAV distribution allocation scheme can be obtained in the end regardless of the method used.

2.1.3 Algorithm solving steps

For the mathematical model constructed in this paper, MATLAB is used to write the code to meet the model requirements, and the following solution steps are designed:

(1) Solving steps for disallowing transit

Calculate the distance from the relief point to each demand point as well as between each demand point, and then calculate the flight time of the UAV from the relief point to each demand location through the flight speed of the UAV, so as to obtain the ensemble of flight time of the UAV from one demand point to any other demand point.

Initially, a material distribution quantity is assigned to each demand point according to the probability formula of the ant colony algorithm within the load range of the UAV. The formula is:

$$P_s^k = \frac{(\tau_s)^\alpha (\eta_s)^\beta}{\sum_{s=1}^{C_{\max}} (\tau_s)^\alpha \cdot (\eta_s)^\beta} \tag{9}$$

$$\eta_s = \frac{1}{|s - C_{\max}|} \tag{10}$$

where P_s^k denotes the probability that the k th ant chooses the drone to carry s pieces of supplies, α is the pheromone heuristic factor, which denotes the importance of the pheromone, β is the heuristic function heuristic factor, which denotes the importance of the heuristic function, s is the number of rescue supplies that each drone chooses to carry on each mission, η_s is the heuristic function, and τ_s is the pheromone concentration of the ants choosing the drone to carry s pieces of supplies, which is calculated as:

$$\tau_s = (1-\rho) \cdot \tau_s + \Delta\tau_s \tag{11}$$

$$\Delta\tau_s = \sum_{k=1}^{m} \Delta\tau_s^k \tag{12}$$

$$\Delta\tau_s^k = \frac{Q}{t_k} \tag{13}$$

m is the number of ants, ρ is the volatilization factor of the pheromone, Q denotes the total amount of pheromone, and t_k denotes the time taken for such selection.

(2) Solving step of allowing transit

The solution step of allowing transit is similar to that of disallowing transit, the difference is that in the third step, in addition to judging whether each demand point completes the task, it is also necessary to calculate whether there is excess material available for transit, and whether the range of the drone is sufficient to support re-distribution, so that the material that meets the conditions for transit will be transit, and the rest of the steps are the same.

2.2 eVTOL Multi-Aircraft Collaborative Trajectory Planning Model

According to the previously mentioned upper layer model to solve the eVTOL multi-machine emergency distribution task allocation, the lower layer model eVTOL multi-machine static coordinated trajectory planning needs to be carried out in the environment where the threat distribution, terrain, and its own performance constraints have been determined on the way to the disaster area, to obtain the minimum comprehensive cost trajectory, and to arrive at the end point safely in accordance with the requirements of the spatio-temporal coordination.

2.2.1 Modeling of spatio-temporal synergistic mechanisms

Planning for eVTOL multi-UAV cooperative trajectories requires a cooperative model. The spatio-temporal synergy cost function of multi-UAV 4D (i.e., 3D spatial dimension + time dimension) trajectories used in this paper is designed as the sum of the time domain synergy cost function and the air domain synergy cost function. Both are calculated as follows.

(1) Time domain synergy mechanism

Multiple emergency logistics UAVs should fly along the planned path from different starting points and arrive at the same mission target point at the same time, which means they should have the same estimated time of arrival (ETA). In addition, the total flight time of the UAVs should be as low as possible to minimize their exposure to threats. In order to determine the globally optimal flight time for multiple UAVs, both the length of the planned path and the flight speed need to be taken into account. The UAV 4D trajectory planning idea can be used to establish a spatio-temporal cooperative mechanism.

Since for any UAV i, its actual flight speed is in a certain range, i.e., $v_{i\min} \le v_i \le v_{i\max}$. Therefore, for a certain distance mission, assuming that the length of the UAV's j th to-be-selected route is L_i^j, and t_i^j denotes the single-path ETA of the UAV's j th to-be-selected route of i, the value of t_i^j is in a certain interval as shown in Eq. (14):

$$t_i^j \in \left[t_{i\min}^j, t_{i\max}^j\right], \text{Which } t_{i\min}^j = \frac{L_i^j}{v_{i\max}}, t_{i\max}^j = \frac{L_i^j}{v_{i\min}} \tag{14}$$

Therefore, for the combined path ETA T_i of UAV i, it should be the concatenated set of ETAs corresponding to each path individually, as shown in Eq. (15):

$$T_i = \left[t_{i\min}^1, t_{i\min}^1\right] \cup \left[t_{i\min}^2, t_{i\min}^2\right] \cup \cdots \cup \left[t_{i\min}^m, t_{i\min}^m\right] \tag{15}$$

For N UAVs, the ETA time-domain cooperative range T is related to T_i as follows:

$$T = T_1 \bigcap T_2 \bigcap \cdots \bigcap T_N \tag{16}$$

For example, the temporal synergy of 3 UAVs is shown in Fig. 2.

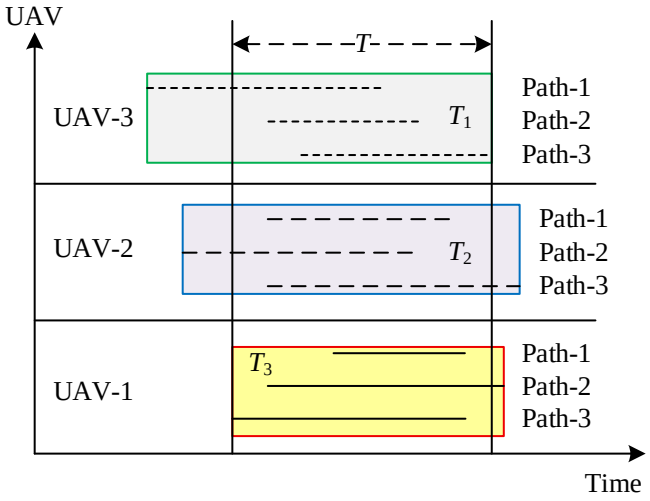

Figure 2: Time coordination diagram

If T is null, it is necessary to re-intersect the alternative trajectories for the UAVs that do not intersect with any of the other UAVs' ETA times, and continue to intersect the combined path ETAs of the remaining UAVs according to the above equation to compute the ETA time-domain synergy range. If there exists a solution to the problem, then T is not empty, and there exists a certain moment t_{ETA} within T such that all drones within the planning range have at least one alternative path that can be satisfied to arrive at the target point at the moment of t_{ETA}, and t_{ETA} denotes the time-domain synergistic ETA, and drone i corresponds to The average speed of its own to-be-selected path j is shown in Eq. (17):

$$v_i^j = \frac{L_i^j}{t_{ETA}} \tag{17}$$

The magnitude of the UAV flight time is the flight time cost. As shown in equation (18), the synergy cost of the UAV is minimized when the time domain synergy ETA takes the minimum value in the set T.

$$J_{ETA} = \min T \tag{18}$$

(2) Airspace synergy mechanism

When planning paths for eVTOL multi-UAVs, it is important to check that each two UAVs are not too close to each other during their flight along their respective paths. The optimal UAV path is necessarily one that completely avoids overlapping collisions in space and time. Given multiple UAVs planning paths, calculating the spacing between any UAV i trajectory and other UAV trajectories at the same moment in time gives:

$$d_{ij}(t) \geq D_{safe} \tag{19}$$

where $d_{ij}(t)$ denotes the trajectory distance between the i and j UAVs at the t moment, and D_{safe} is the safe flight spacing warning threshold between UAVs. The overlapping trajectories of different UAVs have the potential to cause collisions, and the larger the proportion of overlapping trajectory segments, the greater the possibility of collision. Therefore, eVTOL

multi-UAV airspace coordination can be simplified as establishing a mechanism to avoid overlapping trajectories of each UAV. Each track point P of a UAV i's trajectory is compared with each track point q of other UAV trajectories. If the Euclidean distance between the UAV i's waypoint P and the UAV j's waypoint q is less than the minimum safe distance D_{safe}, i.e., $d_{ij}(p,q) < D_{safe}$, it is necessary to further detect whether the arrival times of the corresponding path points are too close together and thus pose a risk. Setting the minimum safe time interval T_{safe}, then at this point, the time intervals between the two UAVs to the points P and q should satisfy $t_{ij}(p,q) \geq T_{safe}$, in order to ensure the safety of the flight.

Therefore, the airspace cooperative safety cost J_{space} can be expressed as equation (20):

$$J_{space} = \begin{cases} \sum_i \sum_{j \neq i} \left(\sum_p \sum_q \frac{1}{d_{ij}(p,q)} + \frac{1}{t_{ij}(p,q)} \right), \\ if\ d_{ij}(p,q) < D_{safe}, t_{ij}(p,q) < T_{safe} \\ 0, otherwise. \end{cases} \tag{20}$$

Combined with the time-domain synergistic cost function, the spatio-temporal synergistic cost of the UAV trajectory J_{ts} is calculated as in Eq. (21):

$$J_{ts} = J_{ETA} + J_{space} \tag{21}$$

2.2.2 Multi-aircraft static cooperative trajectory planning objectives

Combining the task allocation scheme given by the upper model, and the established spatio-temporal cooperative mechanism model, and synthesizing the corresponding penalty functions of the above models, the quality of the UAV's to-be-selected paths can be evaluated in general. Therefore, after normalization, the total objective function of eVTOL multi-aircraft cooperative trajectory planning is established, as shown in Eq. (22):

$$\min f = \sum_{i=1}^{N} J(i) + J_{ts} = \sum_{i=1}^{N} J(i) + J_{ETA} + J_{space} \tag{22}$$

where, $\sum_{i=1}^{N} J(i)$ denotes the total penalty function corresponding to all UAVs in the planning range based on environmental threats, and their own performance limitation constraints, J_{ts} denotes the eVTOL multi-copter cooperative trajectory spatio-temporal cost, J_{ETA} denotes the eVTOL multi-copter cooperative trajectory spatio-temporal cost, and J_{space} denotes the eVTOL multi-copter cooperative trajectory airspace cost.

2.2.3 Quantum Genetic Algorithm

Assuming that the number of target points to be detected by UAVs is N and the number of UAV bases is M. To assign N target points to M UAV bases, the solution space is very huge, which

is difficult to be solved by conventional algorithms, so in this paper, the optimal solution is explored by utilizing the quantum genetic algorithm.

The essence of quantum computing is a probabilistic algorithm, which is a kind of computing method combining the idea of quantum mechanics and the principle of algorithm, at the same time, quantum computing applies the principle of superposition of quantum states, coherence and the concept of quantum entanglement to the algorithm, which improves the parallel efficiency of the algorithm operation and the computational performance.

(1) Principle of Quantum Genetic Algorithm

Quantum Genetic Algorithm (QGA) encodes the chromosomes through the concept of quantum bits and updates the chromosomes using quantum rotating gates, which makes the quantum genetic algorithm characterized by quantum computing. A gene position in a quantum genetic algorithm corresponds to a quantum bit; therefore, the quantum bit needs to contain the full meaning of the gene, and the manipulation of the gene affects the direction of evolution. A gene state can be expressed as $|\psi\rangle = \alpha|0\rangle + \beta|1\rangle$, where α and β are the probability amplitudes of the states $|0\rangle$ and $|1\rangle$ probability amplitudes and satisfy the square normalization condition $|\alpha|^2 + |\beta|^2 = 1$. where $|\alpha|^2$ denotes the probability that the collapse results in 0, and $|\beta|^2$ denotes the probability that the collapse results in 1. A n-bit quantum chromosome can be represented as:

$$\begin{bmatrix} \alpha_1 | \alpha_2 | \cdots | \alpha_n \\ \beta_1 | \beta_2 | \cdots | \beta_n \end{bmatrix} \tag{23}$$

This chromosome can represent 2^n states with $|\alpha_i|^2 + |\beta_i|^2 = 1$ and $i = 1, 2, \cdots, n$, e.g., a chromosome with a number of quantum bits of 3 can be represented:

$$\begin{bmatrix} \frac{1}{\sqrt{2}} & \frac{1}{\sqrt{2}} & \frac{1}{2} \\ \frac{1}{\sqrt{2}} & -\frac{1}{\sqrt{2}} & \frac{\sqrt{3}}{2} \end{bmatrix} \tag{24}$$

The quantum state of this quantum chromosome can be expressed as:

$$\begin{aligned} &\frac{1}{4}|000\rangle + \frac{\sqrt{3}}{4}|001\rangle - \frac{1}{4}|010\rangle - \frac{\sqrt{3}}{4}|011\rangle + \frac{1}{4}|100\rangle \\ &+ \frac{\sqrt{3}}{4}|101\rangle - \frac{1}{4}|110\rangle - \frac{\sqrt{3}}{4}|111\rangle \end{aligned} \tag{25}$$

The above equation represents the state information containing 8 quantum positions, each with probability: 2/16, 1/16, 1/16, 2/16, 3/16, 2/16, 2/16, 3/16, respectively.

The operator that maintains orthogonal normalization transformations of quantum states is a quantum gate. Quantum genetic algorithms transform quantum chromosomes by means of quantum gates, so that the probability amplitude of the quantum bits changes and the transformed to chromosomes also satisfy square normalization. Using this feature of quantum gates can be used to update the chromosomes, and during the updating process, the optimal

chromosome of the parent will affect the evolutionary direction of the chromosomes of the offspring.

A commonly used quantum gate is the quantum rotating gate $U_n = \begin{bmatrix} \cos\theta & -\sin\theta \\ \sin\theta & \cos\theta \end{bmatrix}$, with θ being the angle of rotation, and the updating process of a quantum bit through the quantum gate is shown in Equation (26):

$$\begin{bmatrix} \alpha_i' \\ \beta_i' \end{bmatrix} = U_H(\theta) \begin{bmatrix} \alpha_i \\ \beta_i \end{bmatrix} = \begin{bmatrix} \cos\theta & -\sin\theta \\ \sin\theta & \cos\theta \end{bmatrix} \cdot \begin{bmatrix} \alpha_i \\ \beta_i \end{bmatrix} \tag{26}$$

U denotes the quantum gate, $[\alpha_i, \beta_i]^T$ is the probability amplitude of the i th quantum bit of the chromosome, and $[\alpha_i', \beta_i']^T$ is the probability amplitude after the quantum gate transformation. It can be seen from Eq. The sign of the rotation angle determines the rotation direction of the quantum gate, and the size of the rotation angle θ will determine the convergence speed of the algorithm, so the parameters of the quantum rotating gate are very important for the algorithm to converge, and too large a value of θ will lead to a decrease in the algorithm's accuracy, and too small a value of θ will increase the time of searching for the optimal, and the algorithm will be less efficient. When the quantum bit is in the first and third quadrant, if the sign of the rotation angle is positive, the probability amplitude of the result of the quantum bit collapse after the update is 1 is larger. If the sign of the rotation angle is negative, the probability amplitude of the result of the updated quantum bit collapse is 0 is larger. Conversely, when the quantum bit is in the second and fourth quadrants, if the sign of the rotation angle is positive, the probability amplitude of the result of the post-update quantum bit collapse is 0 is larger. If the sign of the rotation angle is negative, the probability amplitude of the updated quantum bit collapse result is 1 is larger, and the schematic diagram of the quantum revolving door is shown in Fig. 3.

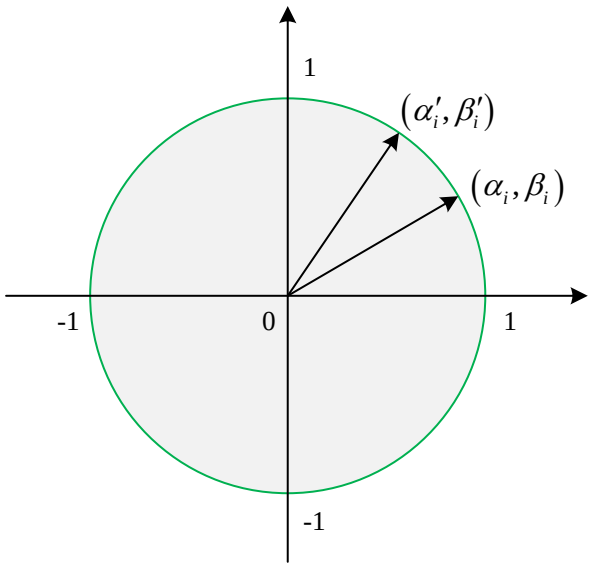

Figure 3: Quantum revolving door

(2) Quantum Genetic Algorithm Process

Initialization. According to the structure of the solution to the problem, construct the initial population $Q(t)=\{q_1^t,q_2^t,\cdots,q_n^t\}$ with a population size of n using the quantum bit encoding form, t is the number of evolutionary generations of the current population, and q_j^t is the j th chromosome in the population of the t th generation:

$$q_j^t=\begin{bmatrix}\alpha_{j1}^t & \alpha_{j2}^t & \cdots & \alpha_{jm}^t\\ \beta_{j1}^t & \beta_{j2}^t & \cdots & \beta_{jm}^t\end{bmatrix},\ j=1,2,\cdots,n \tag{27}$$

where m is the chromosome length, and its value needs to be determined according to the solution of the optimization problem. The population size can be set in a small range due to the parallel optimization search feature of quantum genetic algorithm. The initialization produces chromosomes with equal probability amplitudes of 0 and 1. Both α_{ji}^0 and β_{ji}^0 in the gene take the value of $1/\sqrt{2}$.

Quantum collapse. Quantum collapse is essentially the process of observing a quantum chromosome, i.e., determining the result of the collapse of a quantum chromosome. All individuals within a population $Q(t)$ are measured according to probability amplitudes of 0 and 1, and the result is a determined set of solutions $P(t)$, $P(t)=(X_1^t,X_2^t,\cdots,X_n^t)$. The quantum collapse outcome is determined based on the magnitude of the probability amplitude, assuming that the j th individual is $X_j^t=\{x_{j1}^t,x_{j2}^t,\cdots,x_{jm}^t\}$, $x_{jk}^t\in\{0,1\}$, and $k=1,2,\cdots,m$, and that for this chromosome, the specific method of quantum collapse is to Generate a random vector $S=\{s_1,s_2,\cdots,s_n\}$ containing N random numbers, $s_i\in(0,1)$, $i=1,2,\cdots,m$, and compare s_i and $\left|\alpha_{ji}^t\right|^2$ sequentially if $s_i>\left|\alpha_{ji}^t\right|^2$, then $x_{ji}^t=1$, otherwise $x_{ji}^t=0$.

Calculation of fitness. The fitness $fitness$ of a chromosome is an indicator for assessing the degree of merit of an individual X, and the individual fitness will have an impact on the evolutionary direction of the subsequent individuals. The fitness value needs to be determined based on the optimization direction of the objective function. If the optimization problem requires solving the very small value of the objective function, the fitness $fitness(x)=1/f(x)$, if the optimization problem requires solving the very large value of the objective function, the fitness function can be taken as $fitness(x)=f(x)$.

Quantum Revolving Door Updates. The evolutionary process of an individual in a quantum genetic algorithm requires updating the probability amplitude of genes in an individual through a quantum revolving door. Table 1 shows the quantum rotation angle adjustment strategy, the size and direction of the rotation angle of the quantum revolving door can be determined according to it. In the table, x_{ji}^t denotes the i th quantum position of the solution X_j^t, and b_i^t denotes the i th quantum position of the best adapted solution b^t in the current population. $f(X_j^t)$ and $f(b^t)$ are the fitness of individuals X_j^t and b^t, respectively. $\Delta\theta_i$ is the magnitude of the rotation angle of the quantum revolving door, which is usually taken as 0.01π, α_{ji}^t and β_{ji}^t denote the magnitude of the probability amplitude of the i quantum bit in the j chromosome, respectively, and $s(\alpha_{ji}^t,\beta_{ji}^t)$ denotes the direction of rotation of the quantum bit during the update process, and the rotation angle $\theta_i=s(\alpha_{ji}^t,\beta_{ji}^t)\Delta\theta_i$.

Table 1: Quantum rotation Angle adjustment strategy

x_{ji}^t	b_i^t	$f(X_j^t) \le f(b^t)$	$\Delta\theta_i$	$\alpha_{ji}^t \beta_{ji}^t > 0$	$\alpha_{ji}^t \beta_{ji}^t < 0$	$\alpha_{ji}^t = 0$	$\beta_{ji}^t = 0$
1	1	False	0	0	0	0	0
1	1	True	0	0	0	0	0
1	0	False	0	0	0	0	0
1	0	True	0.01π	-1	+1	±1	0
0	1	False	0	0	0	0	0
0	1	True	0.01π	+1	-1	0	±1
0	0	False	0	0	0	0	0
0	0	True	0	0	0	0	0

When $x_{ji}^t = 0$ and $b_i^t = 1$, if $f(X_j^t) \le f(b^t)$, in order for the updated quantum bits to evolve in the direction of higher fitness, then the value of $\left|\beta_{ji}^t\right|$ should be increased to increase the probability that the result of the collapse of the i th quantum bit in the current solution is 1. At this time, if $(\alpha_{ji}^t, \beta_{ji}^t)$ is in the first or third quadrant, the updating process should be rotated in the counterclockwise direction, i.e., the value of θ_i should be greater than 0. On the contrary, if it is in the second or fourth quadrant, the updating process should be rotated in the clockwise direction, i.e., the value of θ_i should be less than 0.

The flow of quantum genetic algorithm is shown in Fig. 4. Quantum genetic algorithm has strong generality, the algorithm principle is simple, easy to implement, the population has good dispersion, the smaller size of the population can represent more than one solution scheme, the search process is a group parallel search, the global search ability is strong, and the use of collaborative search technology, the use of the current optimal solution of the individual information as the direction of evolution, convergence speed is fast, and is suitable for solving large-scale complex problems.

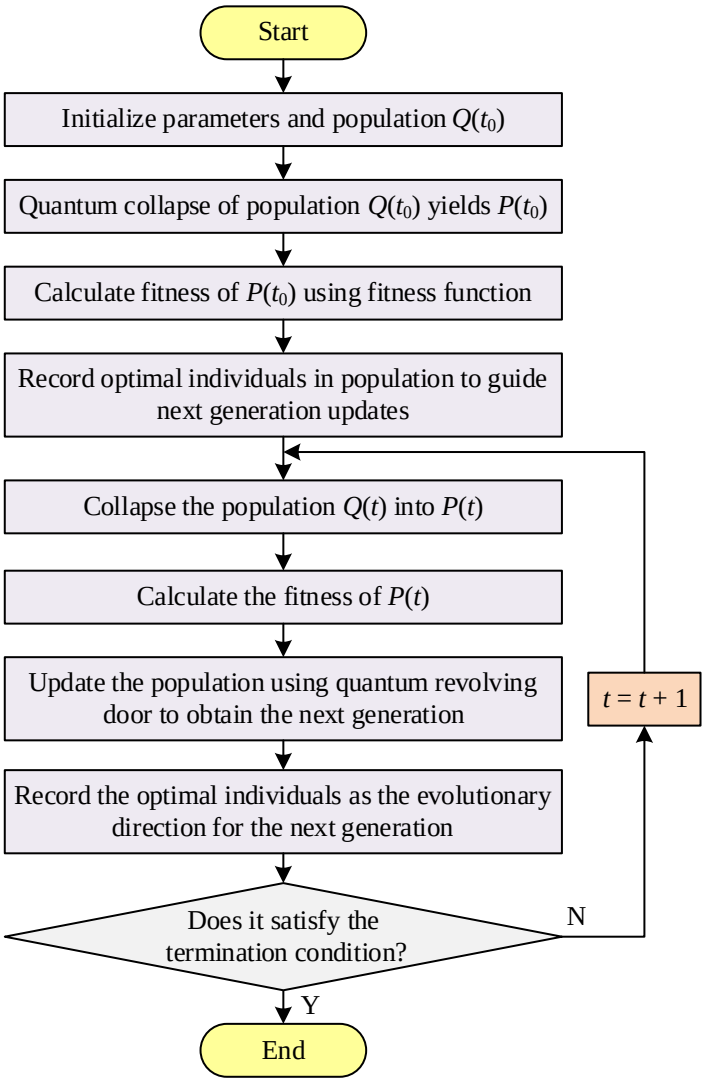

Figure 4: Quantum genetic algorithm process

3 Simulation analysis

3.1 Simulation analysis of eVTOL multi-machine task assignment

All experiments in this chapter were conducted on a computer running Windows 10 Professional 64-bit operating system with a processor configuration of Intel(R) Xeon(R) E-2224 CPU @ 3.40 GHz and 16.0 GB of RAM.All experiments were conducted based on the MATLAB platform with MATLAB version 9.11. 01769968 (R2021b). In this environment, the performance of the proposed algorithm was tested and evaluated.

In order to test the performance of the task allocation algorithm based on the ant colony algorithm for the upper layer model in this paper, we have selected five standard TSP problem instances for testing. These selected problem instances have different path sizes. The five TSP problem instances are Ulysses16, Chn31, Att48, Eil51, and Eil76. Compare GA, GWO with the upper level model of this paper. We ran each problem instance 40 times and the test results are shown in Table 2. The optimal value obtained by GWO and this paper's method in the Ulysses16 instance is the same, 71.847. Other than that, the results obtained by this paper's method in the

other instances are better than the GA and GWO algorithms. And the result of GWO is better than GA.

Table 2: Algorithm comparison

Algorithm		Ulysses16	Chn31	Att48	Eil51	Eil76
GA	Optimal value	73.661	15602.938	35063.293	461.961	570.287
	Mean value	74.636	15681.890	35608.196	469.509	577.751
	Worst value	75.765	15989.605	36094.574	481.235	579.456
GWO	Optimal value	71.847	15605.033	34225.183	456.036	565.801
	Mean value	74.223	16166.394	35932.824	461.788	576.919
	Worst value	75.036	16631.436	37115.576	470.178	592.740
Ours	Optimal value	71.847	15473.755	33930.422	442.764	563.913
	Mean value	72.440	15528.702	35003.691	446.564	568.212
	Worst value	73.106	15884.012	35327.234	455.407	579.296

In order to verify the rationality and effectiveness of this paper's task allocation algorithm based on ant colony algorithm in eVTOL multi-UAV system, GWO algorithm is chosen as a comparison. Simulation experiments were conducted using MATLAB2021b. The algorithm takes the parameter ε=0.2, learning rate η=0.4, and neighborhood radius is γ=2.5.Firstly, we set up a complex eVTOL multi-UAV system with 3 fixed-wing UAVs executing 24 target points. For load balancing of mission planning, each UAV is set to execute 8 target points. Fig. 5 shows the initial state of the eVTOL multi-UAV system, the purple dots are the target points of emergency material requirements to be reached by the UAVs, the red circles are the initial positions of the UAVs (material distribution points), and the black rectangles are the obstacles, which have a radius of R = 13.

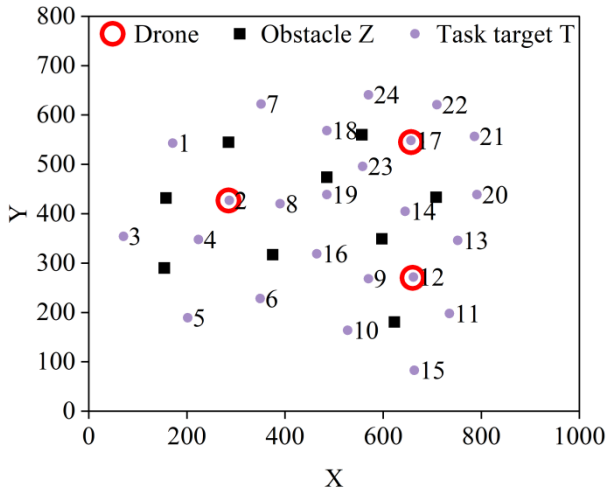

Figure 5: Initial state

Fig. 6 and Fig. 7 show the eVTOL multi-UAV linear paths based on GWO and based on the upper layer model of this paper, respectively, and it can be seen that each UAV can avoid obstacles to reach each target point in turn under both algorithms, but the path trajectory planned by this paper's method is better and smoother. Table 3 shows the values of each parameter of the eVTOL multi-UAV system under the two algorithms. In comparison, the upper layer model of this paper shortens the UAV1, UAV2, and UAV3 paths by 16.67%, 18.87%, and 6.40%, respectively, compared with the UAV1, UAV2, and UAV3 paths planned by GWO. The

simulation experiment results show that the upper layer model in this paper can avoid obstacles to reach the corresponding target point, which is a significant improvement in UAV path optimization.

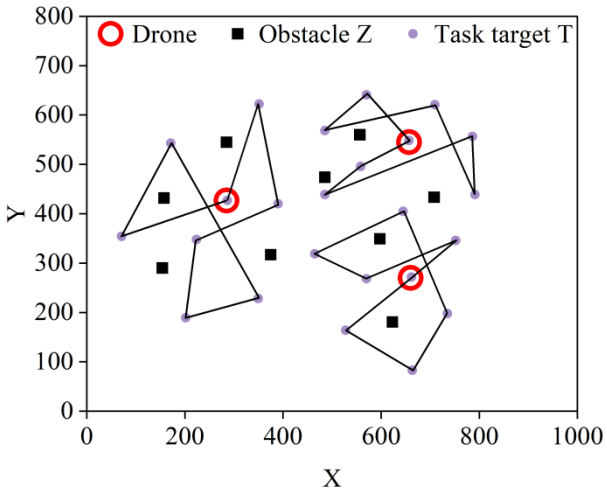

Figure 6: Based on the GWO multiuav line path

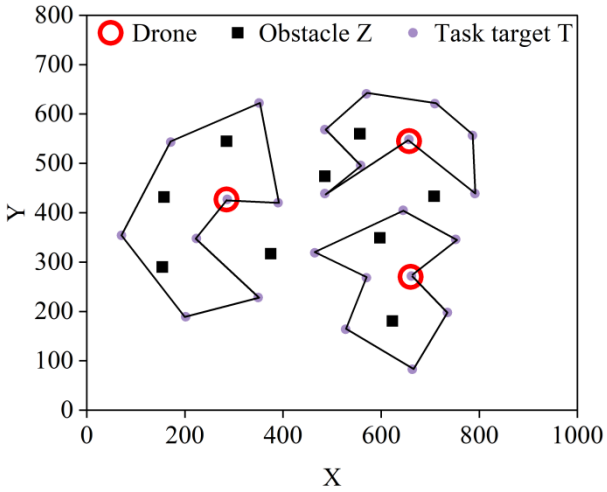

Figure 7: Multi-uav line path of this algorithm

Table 3: Multiple uav system parameters

Algorithm	Path	Landing point	Straight line	Execution sequence
GWO	UAV1	(285,427)	1161.37	2,7,8,4,5,6,1,3,2
	UAV2	(657,545)	1135.42	17,24,18,22,20,21,19,23,17
	UAV3	(660,270)	924.53	12,10,15,11,14,16,9,13,12
Ours	UAV1	(285,427)	967.76	2,8,7,1,3,5,6,4,2
	UAV2	(657,545)	921.18	17,20,21,22,24,18,23,19,17
	UAV3	(660,270)	865.39	12,11,15,10,9,16,14,13,12

In order to more fully verify the performance of the upper layer model in this paper, a part of the algorithms from the international generalized algorithm library VRPLIB is used here for experimental verification. Table 4 provides the linear path comparison data of the five algorithms, and the first column of the table shows the name of a certain algorithm in VRPLIB,

e.g., E016-03m means 3 UAVs and 16 targets. The table details the optimal, mean, median, worst, and standard deviation of the two algorithms for different arithmetic cases and paths, covering the average and minimum time for planning a mission assignment. By comparing the numerical results of the algorithm on these five arithmetic cases, the optimal values of this paper's algorithm on the five arithmetic cases are 223.72, 398.38, 37007.57, 628.82, and 790.79, taking into account the average time and minimum time. The average values are 256.20, 404.30, 37573.89, 650.44, and 939.44, and all the results are superior to the results of the GWO algorithm. The algorithms in this paper show better overall performance in both task assignment and path planning for UAS and the results obtained are more superior.

Table 4: Diameter of the five examples is compared to the data

Numerical example	Algorithm	Optimal value	Mean value	Median value	Worst value	Standard deviation	Mean time (s)	Minimum time (s)
E016-03m	Ours	223.72	256.20	253.54	300.15	29.51	1.081	1.069
	GWO	307.75	328.76	316.09	409.04	33.08	1.057	1.058
E030-04s	Ours	398.38	404.30	496.32	431.67	10.07	1.003	0.941
	GWO	646.81	729.49	717.46	883.12	64.47	0.999	0.994
E048-04y	Ours	37007.57	37573.89	37301.37	38881.01	689.69	1.115	1.057
	GWO	70861.63	80196.24	81611.32	89136.02	6034.81	1.133	1.043
E076-08s	Ours	628.82	650.44	657.38	670.75	22.59	1.142	1.069
	GWO	960.85	1311.45	1319.88	1575.18	217.49	1.107	1.105
E101-08e	Ours	790.79	939.44	961.31	1040.09	84.46	1.119	1.036
	GWO	1526.68	1920.21	2120.88	2306.89	243.41	1.125	1.029

3.2 eVTOL Multi-Aircraft Collaborative Trajectory Planning Simulation Analysis

3.2.1 Simulation Scene Setting

In order to verify the effectiveness of the eVTOL multi-copter cooperative trajectory planning model and algorithm proposed in this paper, the geographic elevation data of Melbourne, Australia is selected for simulation, and the multi-copter simulation scenario is set up as shown in Fig. 8, where there are a total of four different presequence distribution points $D_1 - D_4$, and the common postsequence distribution point is T, whose coordinates are (900,300,25). Four UAVs $U_1 - U_4$ are selected to depart from $D_1 - D_4$ respectively, each UAV has the same estimated takeoff time, and all of them are loaded with goods at the time of departure, and the specific parameters of the UAVs are shown in Table 5, and the parameters of the model and algorithm are shown in Table 6.

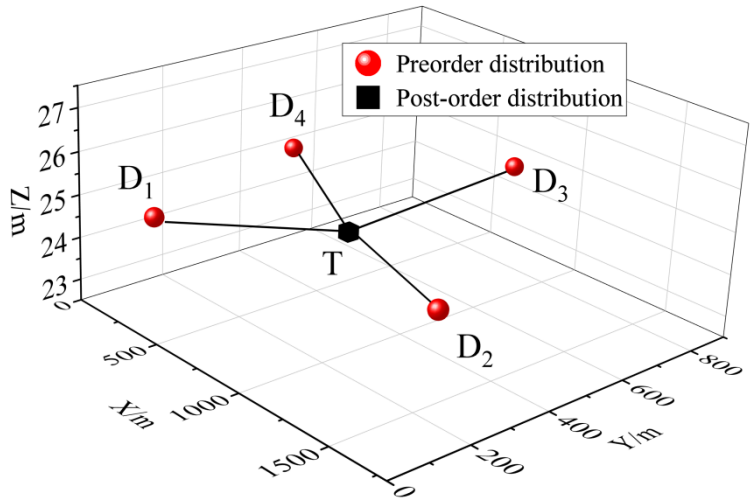

Figure 8: Multi-machine simulation scene setting

Table 5: Unmanned aerial vehicle parameters

Drone code	Preorder distribution D_j /m	Flight range / (m/s)	Maximum range limit $L_{i,\max}$ / km	Maximum take-off quality M_{U_i} / kg	Late arrival T_i^l / s
U_1	(350,50,25)	[10,20]	12	14	70
U_2	(1600,200,25)	[10,15]	8	9	100
U_3	(800,800,25)	[8,17]	6	8	100
U_4	(100,500,25)	[8,17]	10	12	100

Table 6: Model and algorithm parameters

Parameter	Numerical value	Parameter	Numerical value
Weighted coefficient of the coordinated path α_1	0.4	Maximum withstand wind speed $v_{i,w}$	$14\,m/s$
Coordinate time cost weight coefficient α_2	0.6	Arrival time interval S_t	15s
Maximum flight height $H_{\max}$	180m	Search for maximum step $S_{\max}$	15
Minimum flight height $H_{\min}$	15m	Distance threshold d_0	35m
Minimum safety interval $D_{\min}$	10m	Population scale N	200
Equivalent safety level E	1×10^{-5}/h	Genetic algebra	200
Acoustic exposure level limit L_{std}	60dB	Sigmoid function coefficient A	25
Mutation probability P_m	[0.2,0.8]	Cross probability P_c	[0.2,0.6]

3.2.2 Analysis of simulation results

(1) Algorithm performance analysis

15 alternative trajectories are generated for each UAV $U_1 - U_4$ using the eVTOL multi-aircraft collaborative trajectory planning model, which is the lower layer model of this paper, and the planning results of the alternative trajectories are shown in Table 7. Among them, the average value of the trajectory cost of UAV U_3 is optimized to be 0.723, which indicates that the average operation risk, operation noise and transportation cost of its alternative trajectories are at a better level among the UAVs.

Table 7: Alternative route planning results

Drone code	Flight path cost			
	Optimal value	Mean value	Minimum value	Standard deviation
U_1	0.675	0.554	0.151	0.136
U_2	0.598	0.419	0.353	0.049
U_3	0.723	0.705	0.553	0.116
U_4	0.546	0.446	0.136	0.134

The quantum genetic algorithm and GA algorithm are further used to solve the eVTOL multi-copter cooperative trajectory respectively, and the population size N and genetic generations of both algorithms are the same to ensure comparability. In order to reduce the chance of the results, the two algorithms are run 50 times each, and the optimal individual in each run iteration is output as the result of this run, and the results are shown in Table 8. The optimal, average and minimum values of the total cost of eVTOL multicomputer collaboration solved by the quantum genetic algorithm are 0.753, 0.735 and 0.716, which are higher than those of the GA algorithm by 3.72%, 1.66% and 0.28%, respectively, reflecting that the improved algorithm solution results are better than those of the GA algorithm in terms of the optimal, average and worst results. In terms of sub-objective function values, the average values of cooperative trajectory cost and cooperative time cost obtained by the quantum genetic algorithm are 0.654 and 0.816 after normalization of polarity, which are better than the GA algorithm by 3.32% and 1.75%, respectively, which indicate that the eVTOL multi-aircraft cooperative trajectory obtained by the quantum genetic algorithm has better trajectory quality and shorter distribution time, and enhances the safety and safety of eVTOL multi-aircraft emergency delivery in the The safety and distribution efficiency of emergency distribution in the disaster-stricken area are improved, and the multi-objective optimization is better realized.

Table 8: Comparison of coordinated route planning results

Project	Categories	QGA	GA	Rate of change /%
Collaborative trajectory cost	Optimal value	0.655	0.655	0.00
	Mean value	0.654	0.633	3.32
	Minimum value	0.606	0.602	0.66
Collaborative time cost	Optimal value	0.849	0.821	3.41
	Mean value	0.816	0.802	1.75
	Minimum value	0.806	0.792	1.77
Total collaborative cost	Optimal value	0.753	0.726	3.72
	Mean value	0.735	0.723	1.66
	Minimum value	0.716	0.714	0.28

(2) Analysis of optimal solution results

The eVTOL multi-machine cooperative trajectory optimal solution results obtained by quantum genetic and GA algorithms are shown in Table 9. Combined with the alternative trajectory cost of each machine in Table 7, it can be seen that in the cooperative trajectory optimal solution results of the quantum genetic algorithm, the trajectory cost of each UAV obtains the optimal value, while the trajectory cost of UAV U_4 in the GA algorithm is 0.460, which does not take the optimal value, and therefore its relatively poor in terms of risk, noise and transportation cost. In terms of time cost, the flight speed of each UAV planned by quantum genetic algorithm is faster than that of GA algorithm as a whole, which shortens the air flight time and further reduces the overall cooperative time cost of eVTOL multi-copter, and its speed planning results are better.

Table 9: Is the optimal solution for the coordinated navigation

Algorithm	drone	Track price	Time cost	Operating risk	Running noise/dB	Transport cost/yuan	Flight length/s	Planning speed/ (m/s)
QGA	U_1	0.675	0.927	259.471	58.816	0.191	41.5	18
	U_2	0.598	0.759	258.907	62.743	0.193	76.6	14
	U_3	0.723	0.780	126.060	64.389	0.111	91.4	9
	U_4	0.546	0.802	278.840	60.653	0.124	67.2	14
GA	U_1	0.675	0.927	259.471	58.816	0.191	41.5	18
	U_2	0.598	0.735	262.023	62.743	0.193	93.5	13
	U_3	0.723	0.743	129.373	64.389	0.111	67.9	12
	U_4	0.460	0.626	291.986	62.292	0.163	79.7	13

The iterative change curves of the optimal solution results of quantum genetic and GA algorithms corresponding to the total cost of synergy are plotted as shown in Fig. 9. From the optimal value curves, it can be seen that the optimal value of the quantum genetic algorithm population in each generation is higher than that of the GA algorithm, which shows that it is superior to the GA algorithm both in the generation of the initial solution and in the subsequent evolution of chromosome individuals. From the curve of the average value of the total cost of synergy, it can be seen that in the first 1-30 generations of the iteration, the average value of the total cost of synergy of the quantum genetic algorithm population changes more drastically. In the 30-70 generations, the mean curve of the quantum genetic algorithm still fluctuates, while the mean curve of the GA algorithm population has converged to its optimal value, indicating that the GA algorithm population is rapidly controlled by a better individual, and it is easy to fall into the local optimum.

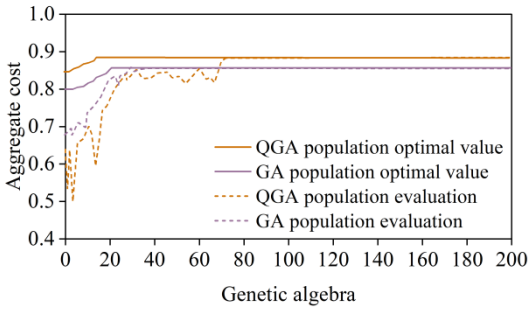

Figure 9: Is the optimal solution and the total cost change curve

3.2.3 Analysis of model parameters

(1) Cost weighting coefficients

When solving the coordinated trajectory of multi-logistics UAVs using quantum genetic algorithm, the value of the weighting coefficient of the objective function $\{\alpha_1, \alpha_2\}$ has a different effect on the solving result. A controlled experiment is used for the analysis, so that the weight coefficient of cooperative trajectory cost α_1 varies sequentially from 0.05 to 1 in steps of 0.05, and the experimental results are shown in Fig. 10. The synergistic trajectory cost shows a trend of increasing and then smoothing, and achieves the maximum value at $\alpha_1 = 0.45$. And the cooperative time cost maintains a high level in the early stage and starts to decrease from α_1=0.65, and also achieves the maximum value at α_1=0.45. Therefore, when α_1=0.45 and α_2=0.65, both the cooperative trajectory cost and the cooperative time cost achieve the optimal result, which is taken as the optimal weight coefficient combination.

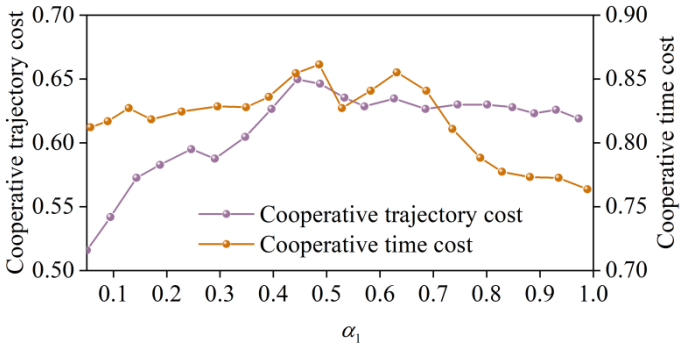

Figure 10: Influenced of the value of weight coefficients on the solution results

(2) Algorithm population size

Under the optimal combination of weight coefficients and arrival time interval, the population size of the quantum genetic algorithm population size varies sequentially from 50 to 400, and the experimental results are shown in Fig. 11. As the population size increases, the total cost of synergy grows rapidly and then remains stable, while the algorithm duration increases linearly. In general, the increase of the population size can get a higher total cost of collaboration, i.e., a better collaborative trajectory planning scheme, but at the same time, the algorithm time also grows accordingly. Considering that the total cost of collaboration tends to stabilize after the population size of 200, the population size of 200 is selected as the optimal population size under the current parameter settings, in order to balance the efficiency and quality of the solution.

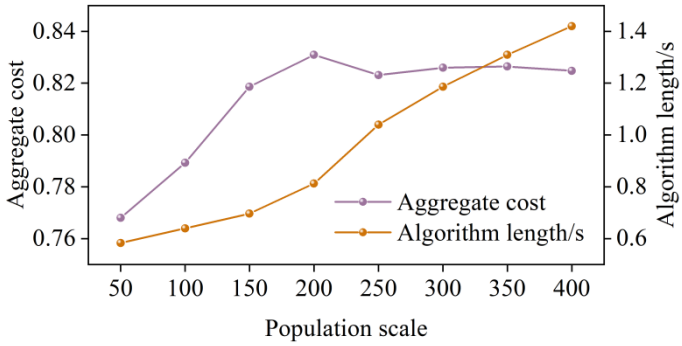

Figure 11: Population size is affected by the solution

4 Conclusion

In this paper, the mutually nested two-layer model is constructed to effectively characterize the interaction between the upper and lower layers, and the ant colony algorithm and quantum genetic algorithm are designed to solve the upper and lower layer models, respectively, which can obtain the effective task allocation and path planning scheme, and provide theoretical guidance for the practice of UAV emergency distribution. The upper layer task allocation model in this paper is better and smoother than all the three paths planned by the GWO algorithm, which are shortened by 16.67%, 18.87% and 6.40% respectively. Using VRPLIB, an international common arithmetic library, for the comparison of arithmetic cases, the optimal and average values of this paper's algorithm on the five cases are better than the solution of GWO algorithm when considering the average time and minimum time. The lower trajectory planning model adopts quantum genetic algorithm, and the algorithm solution performance is the strongest when the weights of cooperative trajectory cost and cooperative time cost are set to 0.45 and 0.65, respectively, and the population size is 200. The optimal, average and minimum values of the total cost of eVTOL multi-machine collaboration solved are higher than those of the GA algorithm by 3.72%, 1.66% and 0.28%, respectively, and the average values of the collaborative trajectory cost and collaborative time cost solved are better than those of the GA algorithm by 3.32% and 1.75%, respectively.

About the Author

Hongyu Jia, born in 1980 in Yuzhou, Henan Province. He is a doctoral candidate in the Service Management program at the Department of Transportation, School of Management, Zhengzhou University. He is also a faculty member at the School of Art and Design, Zhengzhou University of Light Industry. His primary research interests lie in service management and service design.

Jianhua Zhang, born in 1975 in Chengde, Hebei Province. He held a Doctor of Management degree and is currently a professor and doctoral supervisor at Zhengzhou University. His primary research interests lie in the fields of management informatization and knowledge management.

Lulu Zhang, born in 1983 in Zhengzhou, Henan Province. She is an associate professor at the School of Information Engineering, Zhengzhou Institute of Engineering Technology. She held a master's degree from Xi'an University of Science and Technology. Her primary research interests lie in artificial intelligence and wireless communication technology.

Yarui Gao, born in 1982 in Xihua, Henan Province. She is an associate professor and a doctoral candidate in Management Science and Engineering at the School of Management, Zhengzhou University. She is also a faculty member at the School of Economics and Management, Zhengzhou Xiashisai University. Her primary research interests lie in knowledge management and technological innovation.

References

[1] Jiang, Y., Li, X., Zhu, G., Li, H., Deng, J., Han, K., ... & Zhang, R. (2025). Integrated sensing and communication for low altitude economy: Opportunities and challenges. IEEE Communications Magazine.

[2] Ding, J. (2025). Research on the Development of New-Quality Productive Forces Driven by the Low-Altitude Economy under the Coupling of Finance, Technology and Policy.

Asia Pacific Economic and Management Review, 2(5).

[3] WANG, Y., YANG, Y., ZENG, J., HE, Z., & CEN, Z. (2024). Impact of low-altitude technology on low-altitude industry development from perspective of low-altitude economy. Bulletin of Chinese Academy of Sciences (Chinese Version), 40(10), 1853-1866.

[4] Sun, X., Wang, S., Zhang, X., & Wandelt, S. (2025). LAERACE: Taking the policy fast-track towards low-altitude economy. Journal of the Air Transport Research Society, 100058.

[5] Pavel, M. D. (2022). Understanding the control characteristics of electric vertical take-off and landing (eVTOL) aircraft for urban air mobility. Aerospace Science and Technology, 125, 107143.

[6] Bacchini, A., & Cestino, E. (2020). Key aspects of electric vertical take-off and landing conceptual design. Proceedings of the Institution of Mechanical Engineers, Part G: Journal of Aerospace Engineering, 234(3), 774-787.

[7] Zhou, Y. (2025). Unmanned aerial vehicles based low-altitude economy with lifecycle techno-economic-environmental analysis for sustainable and smart cities. Journal of Cleaner Production, 145050.

[8] Kraenzler, M., Schmitt, M., & Stumpf, E. (2019). Conceptual design study on electrical vertical take off and landing aircraft for urban air mobility applications. In AIAA Aviation 2019 forum (p. 3124).

[9] Meng, Z., Ji, J., Liu, L., Liu, S., Sun, Z., Xiao, Q., & Yang, Z. (2025). eVTOL aircraft for the low-altitude economy: A review of development history, core technologies, and future trends. Case Studies on Transport Policy, 101629.

[10] Yan, G., Li, G., & Si, X. (2025, June). Review and Innovation of Traffic Management from the Perspective of Low-Altitude Economy. In 2025 32nd International Conference on Geoinformatics (pp. 1-6). IEEE.

[11] Huang, H., Su, J., & Wang, F. Y. (2024). The potential of low-altitude airspace: The future of urban air transportation. IEEE Transactions on Intelligent Vehicles.

[12] Vieira, D. R., Silva, D., & Bravo, A. (2019). Electric VTOL aircraft: the future of urban air mobility (background, advantages and challenges). International Journal of Sustainable Aviation, 5(2), 101-118.

[13] Liang, S., Wu, X., Wu, Z., & Liu, W. (2025). Progress and Challenges on Materials Used to Optimize Flight Efficiency, Improve Safety and Reliability, and Reduce Cost of Electric Vertical Take-Off and Landing Aircraft. Journal of Applied Polymer Science, 142(24), e57029.

[14] Hu, L., Yan, X., & Yuan, Y. (2025). Development and challenges of autonomous electric vertical take-off and landing aircraft. Heliyon, 11(1).

[15] Jarin, J. B., Beddok, S., & Haritchabalet, C. (2024). Techno-economic comparison of low-

carbon energy carriers based on electricity for air mobility. Energies, 17(5), 1151.

[16] Ison, D. (2024). Consumer willingness to fly on advanced air mobility (AAM) electric vertical takeoff and landing (eVTOL) aircraft. The Collegiate Aviation Review International, 42(1).

[17] Bridgelall, R., White, S., & Tolliver, D. (2023). Integrating electric vertical takeoff and landing aircraft into public airspace: A scenario study. Future Transportation, 3(3), 1029-1045.

[18] Goyal, R., & Cohen, A. (2022). Advanced air mobility: Opportunities and challenges deploying eVTOLs for air ambulance service. Applied Sciences, 12(3), 1183.

[19] Angelini, D., Cestino, E., Cestino, D., & Cattel, F. (2024). Comparative Analysis of eVTOL, Drone, and Ground Transportation Systems for Emergency Delivery of Blood-Derived Medication. In ICAS PROCEEDINGS. ICAS PROCEEDINGS 34th Congress of the International Council of the Aeronautical Sciences Florence, Italy.

[20] Souza, G. O. D., Silva, E. J. D., & Caetano, M. (2025). A Spatial Assessment of eVTOLs for Emergency Medical Transport in the Brazilian Amazon. Journal of Aerospace Technology and Management, 17, e4025.

[21] Espejo-Díaz, J. A., Alfonso-Lizarazo, E., & Montoya-Torres, J. R. (2023). Improving access to emergency medical services using advanced air mobility vehicles. Flexible Services and Manufacturing Journal, 1-33.

[22] Liu, H., Sun, Y., Pan, N., Li, Y., An, Y., & Pan, D. (2022). Study on the optimization of urban emergency supplies distribution paths for epidemic outbreaks. Computers & Operations Research, 146, 105912.

[23] Li, T., Du, Y., Zhang, Z., & Wang, Y. (2025). eVTOL Dispatch Cost Optimization Under Time-Varying Low-Altitude Delivery Demand. World Electric Vehicle Journal, 16(4), 220.

[24] Ganić, E., Barrado, C., Krstić Simić, T., Kuljanin, J., & Baena, M. (2025). Unmanned Aircraft for Emergency Deliveries Between Hospitals in Madrid: Estimating Time Savings and Predictability. Drones, 9(11), 728.

[25] Marzouk, O. A. (2025). Aerial e-mobility perspective: Anticipated designs and operational capabilities of eVTOL urban air mobility (UAM) aircraft. Edelweiss Applied Science and Technology, 9(1), 413-442.

[26] Chen, J., Liu, Y., Chen, X., Tang, L., & Xiong, Z. (2025). Dynamic Takeoff and Landing Control for Multi-Rotor eVTOL Aircraft. International Journal of Aeronautical and Space Sciences, 26(1), 376-389.

[27] Chauhan, S. S., & Martins, J. R. (2020). Tilt-wing eVTOL takeoff trajectory optimization. Journal of aircraft, 57(1), 93-112.

[28] Meng, L., Wu, M., Wen, X., Zhou, Z., & Tian, Q. (2025). Optimization of Flight Scheduling in Urban Air Mobility Considering Spatiotemporal Uncertainties. Aerospace,

12(5), 413.

[29] Wei, H., Lou, B., Zhang, Z., Liang, B., Wang, F. Y., & Lv, C. (2024). Autonomous navigation for eVTOL: Review and future perspectives. IEEE Transactions on Intelligent Vehicles, 9(2), 4145-4171.

[30] Xia, C., Yongtai, L., Liyuan, Y., & Lijie, Q. (2020). Cooperative task assignment and track planning for multi-UAV attack mobile targets. Journal of Intelligent & Robotic Systems, 100(3), 1383-1400.

[31] Wang, Y., Li, J., Yang, X., & Peng, Q. (2025). UAV–Ground Vehicle Collaborative Delivery in Emergency Response: A Review of Key Technologies and Future Trends. Applied Sciences, 15(17), 9803.

[32] Cao, M., Peng, J., Yang, L., & Yang, Y. (2025). Multi-UAV task allocation and path planning in emergency rescue scenarios with uncertain requirements. Journal of Industrial and Management Optimization, 21(10), 6107-6133.